



# Development and validation of an LC-MS/MS method for the quantification of KRAS<sup>G12C</sup> inhibitor opnurasib in several mouse matrices and its application in a pharmacokinetic mouse study

Irene A. Retmana<sup>a,b,\*</sup>, Nefise Çelebi<sup>b</sup>, Jamie Rijmers<sup>a</sup>, Alfred H. Schinkel<sup>a</sup>, Jos H. Beijnen<sup>c,d</sup>, Rolf W. Sparidans<sup>b</sup>

<sup>a</sup> The Netherlands Cancer Institute, Division of Pharmacology, Plesmanlaan 121, 1066 CX Amsterdam, The Netherlands

<sup>b</sup> Utrecht University, Faculty of Science, Department of Pharmaceutical Sciences, Division of Pharmacology, Universiteitsweg 99, 3584 CG, Utrecht, The Netherlands

<sup>c</sup> The Netherlands Cancer Institute, Department of Pharmacy & Pharmacology, Plesmanlaan 121, 1066 CX Amsterdam, The Netherlands

<sup>d</sup> Utrecht University, Faculty of Science, Department of Pharmaceutical Sciences, Division of Pharmacoepidemiology and Clinical Pharmacology, Universiteitsweg 99, 3584 CG Utrecht, The Netherlands

## ARTICLE INFO

### Keywords:

Opnurasib  
KRAS<sup>G12C</sup> inhibitor  
LC-MS/MS  
Bioanalysis  
Mouse matrices

## ABSTRACT

Opnurasib (JDQ-443) is a highly potent and promising KRAS<sup>G12C</sup> inhibitor that is currently under clinical investigation. Results of the ongoing clinical research demonstrated the acceptable safety profile and clinical activity of this drug candidate as a single agent for patients with NSCLC harboring KRAS<sup>G12C</sup> mutations. In this early stage of development, a deeper insight into pharmacokinetic properties in both preclinical and clinical investigations of this drug is very important. Thus, a reliable quantification method is required. To date, no quantitative bioanalytical assay of opnurasib was publicly available. In this study we present a validated assay to quantify opnurasib in mouse plasma and eight mouse tissue-related matrices utilizing liquid chromatography-tandem mass spectrometry. Erlotinib was used as internal standard and acetonitrile was utilized to treat 10 µl of the sample with protein precipitation in a 96-well plate format. Separation and detection were achieved using a BEH C18 column under basic chromatographic conditions and a triple quadrupole mass spectrometer, respectively. We have fully validated this assay for mouse plasma and partially for eight mouse tissue-related matrices over the range of 2–2000 ng/ml. The accuracy and precision of the assay fulfilled international guidelines (EMA & U.S. FDA) over the validated range. The method was proven selective and sensitive to quantify opnurasib down to 2 ng/ml in all investigated matrices. The recoveries of both analyte and internal standard in mouse plasma were ~100 % with no significant matrix effect in any of the matrices. Opnurasib in mouse plasma was stable up to 12 h at room temperature, and up to 8 h at room temperature in tissue homogenates (except for kidney up to 4 h). This presented method has been successfully applied to quantify opnurasib in preclinical samples from a mouse study and demonstrated its usability to support preclinical pharmacokinetic studies.

## 1. Introduction

Kirsten rat sarcoma virus (KRAS) is one of the most often observed

mutated human oncogenes in solid tumors such as lung, colorectal, and pancreatic cancer [1,2]. The association of the presence of mutant KRAS gene with a poor prognosis in patients with non-small cell lung

**Abbreviations:** AUC, Area Under the concentration–time Curve; BEH, Bridged Ethylene Hybrid; BSA, Bovine Serum Albumin; BID, bis in die twice a day; EMA, European Medicines Agency; FVB, Friend Virus B-Type; IS, Internal standard; ISR, Incurred Sample Reanalysis; KRAS, Kirsten Rat Sarcoma; LC, Liquid Chromatography; LC-MS/MS, Liquid Chromatography-tandem Mass Spectrometry; LLOQ, Lower Limit of Quantification; MS, Mass Spectrometry; NSCLC, Non-small Cell Lung Carcinoma; PP, Protein precipitation; QC, Quality Control; SIL, Stable Isotope Labelled; SRM, Selected Reaction Monitoring; ULOQ, Upper Limit of Quantification; US FDA, United States Food and Drug Agency.

\* Corresponding author at: The Netherlands Cancer Institute, Division of Pharmacology, Plesmanlaan 121, 1066 CX Amsterdam, The Netherlands.

E-mail addresses: [i.a.retmana@uu.nl](mailto:i.a.retmana@uu.nl) (I.A. Retmana), [n.celebi@students.uu.nl](mailto:n.celebi@students.uu.nl) (N. Çelebi), [j.rijmers@nki.nl](mailto:j.rijmers@nki.nl) (J. Rijmers), [a.schinkel@nki.nl](mailto:a.schinkel@nki.nl) (A.H. Schinkel), [j.beijnen@nki.nl](mailto:j.beijnen@nki.nl) (J.H. Beijnen), [r.w.sparidans@uu.nl](mailto:r.w.sparidans@uu.nl) (R.W. Sparidans).

<https://doi.org/10.1016/j.jchromb.2023.123964>

Received 25 September 2023; Received in revised form 8 November 2023; Accepted 6 December 2023

Available online 9 December 2023

1570-0232/© 2023 The Authors. Published by Elsevier B.V. This is an open access article under the CC BY license (<http://creativecommons.org/licenses/by/4.0/>).

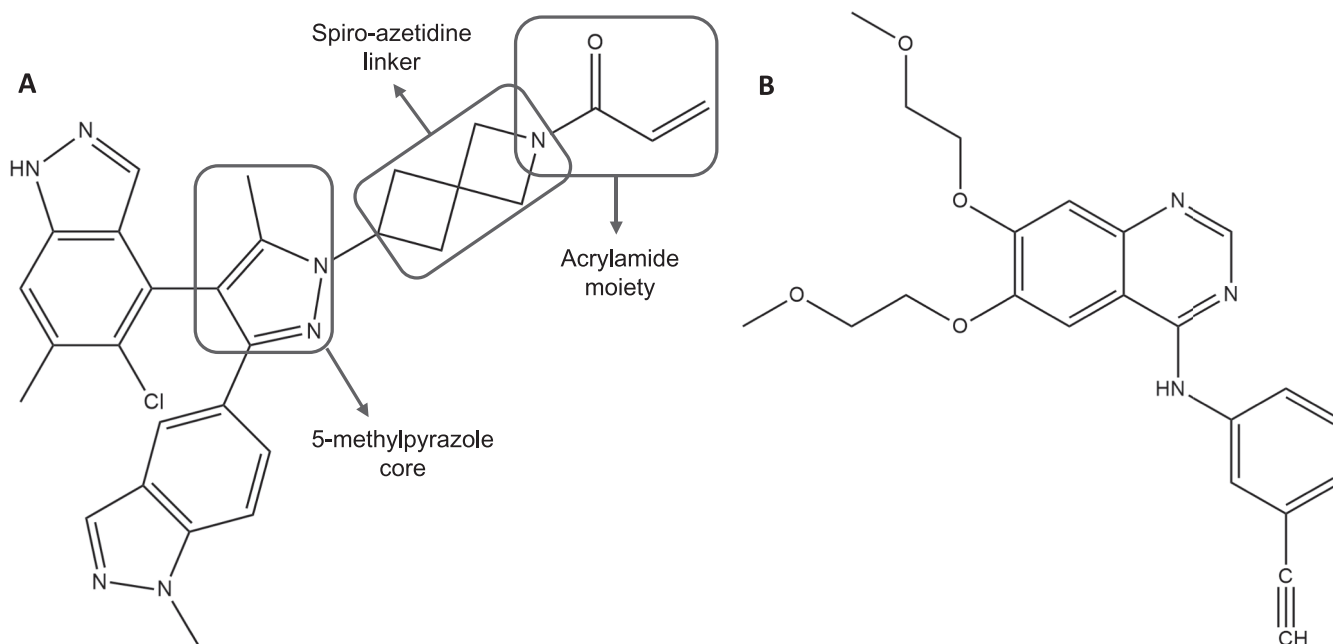


Fig. 1. Molecular structures of opnurasib (A) and erlotinib (internal standard) (B).

carcinoma (NSCLC) has been reported [3,4], indicating the possibility of improvement with a KRAS targeted therapy.

Shokat et al. was the first group introducing the possibility to directly target the long-considered undruggable KRAS<sup>G12C</sup> mutant through covalent inhibition in 2013 [5]. This group also identified the new allosteric pocket beneath the switch II region as the additional target site inhibition. Subsequently, the introduction of the first *in-vivo* active KRAS<sup>G12C</sup> inhibitor ARS-162 in 2018 initiated a new journey of KRAS inhibitors development [6]. Following this step, the approval of KRAS<sup>G12C</sup> inhibitors sotorasib (previously known as AMG510) and adagrasib (previously known as MRTX-849) by the US FDA in 2021 and 2022, respectively, to treat patients with NSCLC highlighted the fast development of KRAS inhibitors [7,8]. Continuing on this momentum, several other promising KRAS<sup>G12C</sup> inhibitors with potent activity both *in vitro* and *in vivo* were developed [9].

One of the promising candidates is opnurasib (also known as JDQ-443). The preclinical investigation of this compound showed a comparable efficacy to sotorasib [10,11]. Opnurasib, similar to sotorasib and adagrasib, has an acrylamide moiety responsible for its covalent engagement with C12 of the KRAS<sup>G12C</sup> protein [11,12]. The differences between opnurasib and its predecessor in its molecular structure is the unique 5-methylpyrazole as its core structure and a spiro-azetidine moiety as its linker to the acrylamide warhead intended to achieve an optimum engagement with its target site (Fig. 1A) [12]. Opnurasib has advanced to an open label phase Ib/II clinical study to assess its safety and tolerability as a single agent and in combination with other therapy to treat advanced solid tumors in patients who harbored the KRAS<sup>G12C</sup> mutation (KontRASt-01, NCT04699188) [13]. An updated result of this ongoing study showed an acceptable safety profile of opnurasib as a single therapy for patients with advanced solid tumors at a dose of 200 mg BID, and it showed clinical activity in patients with NSCLC [14].

Opnurasib is intended as therapy for cancer patients. Such therapies are often characterized by a narrow therapeutic window and the necessity of individual dose adjustment considering the patient's condition to ensure the safety-efficacy balance of the therapy [15,16]. Therefore, a deeper insight into the pharmacokinetic profile both on preclinical and clinical levels is essential. To obtain such knowledge, a reliable quantitative determination of opnurasib in biological samples is crucial. To our knowledge, there is no quantification method for opnurasib

published to date. Therefore, in this study, we aim to provide a quantitative assay of opnurasib in mouse plasma, seven tissue homogenates, and small intestinal content homogenates. This validated bioanalytical assay can be used further to support preclinical investigation of opnurasib to obtain more insight into its pharmacokinetic profile and tissue distribution.

## 2. Material and methods

### 2.1. Chemicals and reagents

Opnurasib (JDQ-443, Mw = 526.03 g/mol, >98 %) was supplied by DC Chemicals (Shanghai, China). Erlotinib (Mw = 393.44 g/mol, as hydrochloric acid, >99 %) as internal standard was obtained from Sequoia Research Products (Pangbourne, UK). ACS grade of ammonium hydroxide solution (28–30 % NH<sub>3</sub> basis) and ACS grade of formic acid (98–100 %), used as pH modifier, were purchased from Sigma-Aldrich (Steinheim, Germany) and Merck (Darmstadt, Germany), respectively. Water (ULC-MS grade), methanol (HPLC grade), and acetonitrile (HPLC grade) were supplied by Biosolve (Valkenswaard, The Netherlands). 2-propanol (analytical grade) was obtained from Serva Electrophoresis (Heidelberg, Germany). Pooled CD-1 mouse lithium heparin plasma (mixed gender) and pooled human lithium heparin plasma (mixed gender) were both acquired from BioIVT (West Sussex, UK).

### 2.2. Analytical instruments

Analytical instruments utilized for quantification of opnurasib were an Infinity II LC (Agilent, Singapore) and a 6475 Triple Quadrupole MS system (Agilent, Singapore). This system consisted of an Infinity II high speed pump, an Infinity II multisampler, an Infinity II multi column thermostat, and a 6475 triple quadrupole mass spectrometer equipped with an Agilent jet stream electrospray source. Mass Hunter work station software consisted of Mass Hunter LC-MS/MS data acquisition version 12.0, Mass Hunter qualitative analysis version 10.0, and Mass Hunter quantitative analysis version 12.0 was used for all data collection and both qualitative and quantitative data processing.

**Table 1**

Individual selected reaction monitoring (SRM) parameters of opnurasib and internal standard erlotinib.

Compound	Q1 ( <i>m/z</i> )	Q3 ( <i>m/z</i> )	Fragmentor (V)	CE (V)
Opnurasib	526.2	79.0*	200	44
		77.0	200	124
Erlotinib	394.2	74.9*	170	124

*m/z* = mass over charge, CE = collision energy, V = volts. \*used for quantification

### 2.3. LC-MS/MS conditions

An Acquity UPLC® BEH C18 column (30 × 2.1 mm,  $d_p = 1.7 \mu\text{m}$ , Waters, Milford, MA, USA) protected with UPLC® BEH C18 Vanguard pre-column (5 × 2.1 mm,  $d_p = 1.7 \mu\text{m}$ , Waters) was utilized as the separation column. The chromatographic eluent consists of water modified with 0.1 % (v/v) ammonium hydroxide and 0.01 % (v/v) formic acid (eluent A) and acetonitrile (eluent B). Eluent A was prepared daily, and its pH was noted (pH range of 9.9–10.0). After an injection of 2.5  $\mu\text{l}$  of sample, a linear gradient at a flow rate of 0.5 ml/min was applied as follows: 0 min, 35 % B; 1.00 min, 70 % B; 1.01 min, 100 % B; 1.50 min, 100 % B; 1.51 min, 35 % B; 2.00 min, 35 % B. Utilizing the divert valve, the whole eluate was transferred to the ionization interface between 0.3 and 1.3 min after the injection. During the analysis, the temperatures of multisampler and thermostat column were maintained at 4 °C and 40 °C, respectively. Selected reaction monitoring (SRM) in the positive ion mode was used as the detection mode with optimized parameters utilizing nitrogen gas: capillary voltage 4,300 V, nozzle voltage 1,500 V, gas temperature 100 °C, gas flow 10 L/min, sheath gas temperature 400 °C, sheath gas flow 12 L/min, and nebulizer gas 25 psi. These parameters were optimized by flow injection analysis (FIA) of 1000 ng/ml opnurasib in a mixture of 0.1 % formic acid in water (v/v) and methanol (2:8, v/v). In short, 0.5  $\mu\text{l}$  of 1000 ng/ml opnurasib was introduced to the column at 0.5 ml/min flow rate of 0.1 % formic acid in water (v/v) – acetonitrile (55:45, v/v) utilizing optimization algorithm options within Mass Hunter software. The individual SRM parameters for both opnurasib and erlotinib (IS) are listed in Table 1.

### 2.4. Stock and working solutions

A stock solution of 0.5 mg/ml of internal standard (IS) was made by dissolving 200–300  $\mu\text{g}$  erlotinib in methanol. A serial dilution of a stock solution with acetonitrile was performed to obtain 1000 ng/ml and 10 ng/ml erlotinib in acetonitrile. The 10 ng/ml of erlotinib in acetonitrile was used as daily IS and precipitating agent.

Two separate stock solutions of 0.5 mg/ml of opnurasib were prepared by dissolving 300–350  $\mu\text{g}$  of opnurasib in methanol. Two subsequent working solutions of 50,000 ng/ml were then made by diluting the stock solution with 50 % (v/v) methanol. These two working solutions were used further to prepare calibration and quality control (QC) samples in mouse plasma independently. All the solutions were stored in the freezer with controlled temperature at –30 °C.

### 2.5. Calibration and quality control samples

The highest calibration sample of 2,000 ng/ml opnurasib was prepared by diluting the first working solution (50,000 ng/ml opnurasib) with blank pooled lithium heparin mouse plasma in a polypropylene tube. The highest calibration sample was diluted further daily to 1000, 200, 100, 20, 10, 5, and 2 ng/ml of opnurasib in blank mouse plasma to be used as daily calibration samples. QC samples were prepared from the second working solution (50,000 ng/ml opnurasib) via a sequential dilution to QC-high (1,500 ng/ml opnurasib), QC-med (150 ng/ml opnurasib), QC-low (6 ng/ml opnurasib), and QC-LLoQ (2 ng/ml opnurasib) in pooled blank mouse plasma. QC-med (150 ng/ml

opnurasib) samples were also prepared in pooled blank mouse tissue-related homogenates of brain, kidney, liver, spleen, small intestines, small intestinal content, lung, and testis for the partial validation in these tissue-related homogenates. The highest calibration and QC samples were stored at –30 °C until further use.

### 2.6. Sample preparation

A protein precipitation method was used to treat all mouse plasma and tissue-related homogenate samples. Shortly, ten  $\mu\text{l}$  of mouse plasma or tissue-related homogenate was pipetted into a 200  $\mu\text{l}$  polypropylene 96-well plate with a conical bottom. Further, a 30  $\mu\text{l}$  IS solution was added to these samples, followed by brief shaking of the closed 96-well plate with a vortex mixer. The plate was then centrifuged at 3500 × g, at a temperature of 20 °C for 5 min with an Heraeus Multifuge 3S-R centrifuge (Kendro laboratory products, Hanau, Germany). Thirty  $\mu\text{l}$  of supernatant was transferred into a 96-deep well polypropylene plate with a round bottom. Next, 150  $\mu\text{l}$  of 25 % methanol (v/v) was added to the deep well, followed by a short gentle shaking of the well plate. The prepared plate was placed in the multisampler for an injection. Finally, 2.5  $\mu\text{l}$  of sample was injected onto the analytical column.

### 2.7. Bioanalytical method validation

Full validation of the quantification method was performed on mouse plasma, while partial validation was conducted for all investigated tissue-related homogenates in the range of 2–2000 ng/ml opnurasib. The validation procedures in this paper follow the latest guidelines on bioanalytical method validation of European Medicine Agency (EMA) [17] and United States Food and Drug Administration (US FDA) [18].

#### 2.7.1. Selectivity

The selectivity of the assay was investigated in six individual blank mouse plasma (non-hemolyzed and non-lipemic) and 32 individual blank tissue-related homogenates (4 individual blanks for each investigated tissue-related) at QC-LLoQ level.

#### 2.7.2. Calibration curve and range

Calibration samples with a range of 2–2,000 ng/ml opnurasib, a blank (IS only), and a double blank (no analyte and no IS) were prepared in pooled lithium heparin mouse plasma. This sample set was daily prepared in duplicate ( $n = 20$ ). The calibration curve was defined by a linear regression of the area ratio of opnurasib/IS against the concentration of opnurasib. The inversed square of the opnurasib concentration was utilized as the weighting factor of the calibration curve.

#### 2.7.3. Accuracy and precision

To define the performance of the assay, accuracy and precision were assessed at four different concentration levels (QC-LLoQ, QC-low, QC-med, and QC-high) in pooled mouse plasma and at one concentration level (QC-med) in all investigated tissue-related homogenates (pooled). Precision and accuracy were determined in sextuple analysis in three independent runs on three different days ( $n = 18$  per QC level). The percentage of coefficient of variance/CV (%) and the percentage of bias/bias (%) determined the precision and accuracy of the method. These two parameters were calculated both intra- and inter-day.

#### 2.7.4. Matrix effect

Similar to selectivity, the matrix effect was investigated in six individual mouse plasma and four individual samples for each tissue-related homogenate. QC-low and QC-high samples were prepared in these individual blank matrices and quadruplicate analysis was performed for each individual matrix. The accuracy and precision were calculated to define the effect of the different sources of matrix on the quantification of opnurasib.

The matrix effect of hemolyzed plasma was investigated in pooled matrix. In short, pooled mouse plasma was spiked with 10 % of pooled mouse hemolyzed whole blood. This matrix was used to prepare QC-low and QC-high samples of opnurasib. The analysis of the effect of hemolyzed matrix was performed in quadruplicate analysis for each QC level.

#### 2.7.5. Recovery

The recovery was investigated by a quadruplicate analysis at QC-low, QC-med, and QC-high samples ( $n = 12$ ) in pooled lithium heparin mouse plasma and pooled lithium heparin mouse plasma.

#### 2.7.6. Carry-over

Carry-over was determined by injecting a blank or double blank sample after the injection of the highest calibration samples. The response at the retention time of opnurasib was recorded (if any) and compared to the response of opnurasib at QC-LLoQ level to determine the carry-over of the method.

#### 2.7.7. Dilution integrity

Dilution integrity was investigated by diluting a mouse plasma sample containing 5000 ng/ml opnurasib with lithium heparin human plasma. The dilution integrity was defined at the dilution factors of 5-fold, 10-fold, 11-fold, and 51-fold ( $n = 6$  for each dilution factor).

#### 2.7.8. Stability

The stability of opnurasib in mouse plasma was investigated at QC-low and QC-high levels ( $n = 4$  for each level). Quadruplicate analysis of each investigated QC-level was performed following sample exposure to room temperature for 6, 8, 12, and 24 h to assess bench top stability. In addition, QC-low and QC-high samples were also exposed to  $-30\text{ }^{\circ}\text{C}$  for 3 months (long term stability) and at  $-30\text{ }^{\circ}\text{C}$  interrupted by three freeze-thaw cycles (thawing at room temperature for 2 h and refreezing at least for 12 h). Meanwhile the stability of opnurasib in tissue-related homogenates was investigated at QC-med level after its exposure to room temperature for 8 h ( $n = 4$  for each tissue-related homogenate) as partial validation of tissue-related homogenates.

The stability of opnurasib in whole blood was also investigated via a sequential dilution of 50,000 ng/ml of opnurasib in 50 % methanol (v/v) with pooled and freshly collected mouse whole blood to obtain QC-high and QC-low samples. These samples were exposed to both room temperature and on ice condition for 30, 60, 120, 180, 240 and 360 min ( $n = 4$  for each exposure time and condition). The whole-blood samples were added with lithium heparin human plasma (10-folds dilution) directly after the exposure time prior to further analysis.

The stability of opnurasib in processed samples was determined by reinjecting the QC-low and QC-high samples after 7 days storage at  $4\text{ }^{\circ}\text{C}$  (multisampler temperature). The stability samples in different matrices and processed samples were calculated by comparing the calculated concentration to its nominal concentration.

The stability of opnurasib in both stock and working solutions was assessed after the exposure to room temperature with the presence of light for 6 h and after 4 months storage at  $-30\text{ }^{\circ}\text{C}$ . The response of these solutions was compared to the response of freshly prepared stock and working solutions at the same level.

#### 2.7.9. Incurred samples reanalysis

A reanalysis of 60 samples from the mouse study ( $n = 12$  for plasma and  $n = 6$  for each investigated tissue-related homogenates) was performed 1 week after the first measurement. In between the two analyses, these samples were stored at  $-30\text{ }^{\circ}\text{C}$ . The percentage of difference of these two independent analyses was calculated and plotted.

### 2.8. Blood-to-plasma concentration ratio ( $R_b$ )

To assess the blood-to-plasma concentration ratio ( $R_b$ ) of opnurasib the mouse whole blood (freshly collected and pooled) was spiked with

opnurasib at 1,500 ng/ml (QC-high). The spiked whole blood was then incubated at  $37\text{ }^{\circ}\text{C}$  for 1 h ( $n = 4$ ). After the incubation, 10  $\mu\text{l}$  of the spiked whole blood was supplemented directly with 90  $\mu\text{l}$  lithium heparin human plasma (WB sample). The remaining spiked whole blood was centrifuged at  $6000 \times g$  speed and temperature of  $4\text{ }^{\circ}\text{C}$  for 6 min to obtain the plasma. The collected plasma (plasma-derived sample) and the WB sample were then further analyzed utilizing the validated method to determine  $R_b$ .

### 2.9. Preclinical study

#### 2.9.1. Mouse treatment

The preclinical study to show the applicability of the method was performed in six male wild-type mice (FVB genetic background) with ages between 8 and 16 weeks. The housing and handling of the mice followed the institutional guidelines of The Netherlands Cancer Institute and complied with the Dutch and EU legislation. The mice received orally administered opnurasib at a dose of 30 mg/kg body weight after they had been fasted for approximately 2–3 h. Their blood was withdrawn from the tail vein at 0.25, 0.5, 1, 2, and 4 h after drug administration ( $\sim 50\text{ }\mu\text{l}$  per sample), using heparinized microvettes. The final blood collection was performed by cardiac puncture eight hours after opnurasib administration. Finally, the mice were sacrificed by cervical dislocation, and the tissues of interest (brain, liver, spleen, kidney, small intestines, lungs, and testis) were immediately harvested. Small intestinal content was also collected during organ harvesting. Plasma samples were obtained from withdrawn blood via centrifugation at 6000 g for 6 min at  $4\text{ }^{\circ}\text{C}$ . All the harvested organs were prepared according to Section 2.9.2. Prior to homogenization with 2 % (w/v) BSA, small intestines and lungs were first rinsed with saline. All samples were stored at  $-30\text{ }^{\circ}\text{C}$  before further quantification. All the plasma samples and liver homogenates were diluted 5 times, while small intestines and small intestinal contents homogenates were diluted 11 times with human lithium heparin plasma before quantitative analysis. The remaining biological matrices were directly prepared according to Section 2.6.

#### 2.9.2. Tissue homogenization

The mouse tissue-related homogenate samples, both blank samples for the validation and preclinical samples, were prepared by mixing the whole harvested organ (weighed) with 2 % (w/v) of bovine serum albumin (BSA) in milli-Q water in an iced condition. The volumes of BSA added for every organ were as follows: 1 ml of BSA solution was used for the brain, spleen, lung, and testis; 2 ml of BSA solution was added for kidney and small intestinal content; 3 ml of BSA solution was used for the liver and small intestines. A FastPrep-24™ 5G instrument (M.P Biomedicals, Santa Ana, USA) was utilized for the homogenization process.

#### 2.9.3. Preclinical data calculation

Microsoft Excel was used to calculate all the corrected concentrations of opnurasib in mouse plasma and mouse tissue obtained from preclinical samples. The pharmacokinetic parameters of opnurasib in individual mouse were calculated utilizing PK Solver 2.0 [19] and further processed in Microsoft Excel to obtain the average and standard deviation for each parameter. The reported pharmacokinetic parameters were calculated following non-compartmental analysis and the area under curve (AUC) was calculated following trapezoidal rules. The concentration of opnurasib in tissue and small intestinal content was calculated based on their individual weights. All the graphs were created utilizing GraphPad Prism 9 (GraphPad Software, La Jolla, CA).

## 3. Results and discussion

To the best of our knowledge this is the first description of a validated quantification method for opnurasib, developed for mouse plasma and several tissue-related homogenates. The described quantification

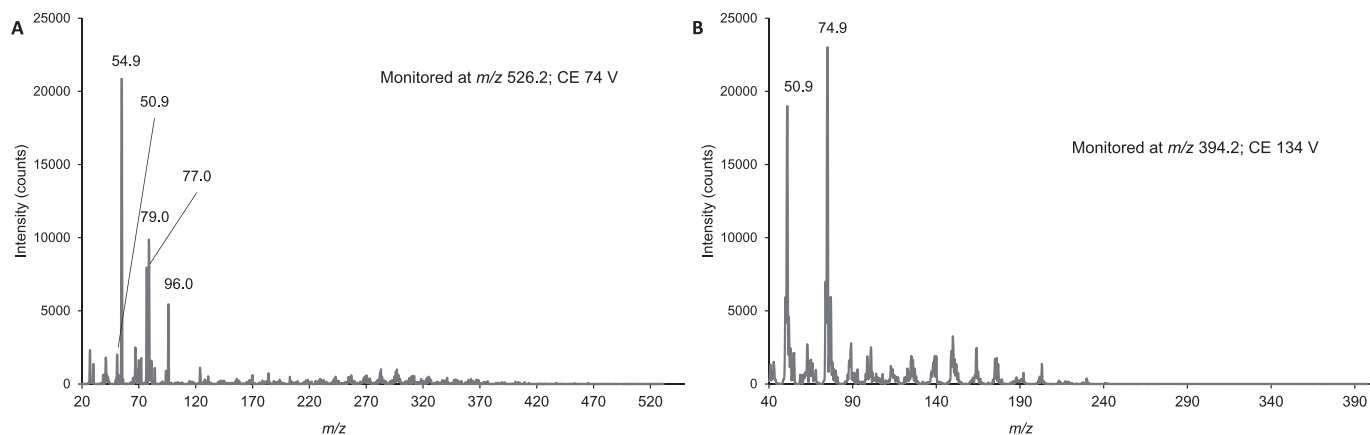


Fig. 2. Product ions of (A) protonated opnurabisib ( $m/z$  526.2) and (B) protonated erlotinib ( $m/z$  394.2). CE = collision energy.

method of opnurabisib is efficient with a two-minute run time preceded by a straightforward protein precipitation to treat all samples. Moreover, we developed this assay specifically for analyzing a small volume of sample (10  $\mu$ l) in a 96-well plate format enabling the possibility of high-throughput analysis and enhancing the applicability of this method to support preclinical studies in a small rodent, specifically a pharmacokinetic study of opnurabisib in mice orally administered with 30 mg/kg body weight of opnurabisib.

### 3.1. Method development

The jet stream ionization was optimized in positive mode for a single protonated opnurabisib ( $m/z = 526.2$ ) to obtain a maximum response. The product masses optimized during the ionization step were  $m/z$  54.9, 77.0, and 79.0. The  $m/z$  79.0 was selected as quantifier due to its lower noise background resulting in higher signal to noise ratio compared to other masses. Similar optimization was also performed for single protonated erlotinib ( $m/z$  394.1), the internal standard. The product ion monitored for erlotinib was  $m/z$  74.9. The product spectra of single protonated opnurabisib and erlotinib are shown in Fig. 2. The fragmentation of protonated opnurabisib into product ion of  $m/z$  79.0 was proposed to follow the protonated benzene contained in its molecular structure (Fig. 1A).

The chromatographic separation was developed and optimized on the Acquity UPLC™ BEH C18 column based on MS response, peak shape, and retention time. Acetonitrile was selected as the organic phase because it offered lower back pressure than methanol in the same

proportion. Both acidic and basic conditions utilizing water modified with either 0.1 % formic acid (v/v, pH 2.8) and 0.1 %  $\text{NH}_4\text{OH}$  (v/v, pH 10.7) were investigated. We observed an approximately 5-fold higher response of opnurabisib in basic than acidic conditions. Since the method sensitivity was crucial for our preclinical samples, we opted to use basic condition to further develop our assay. However, the introduction of biological matrices, *i.e.*, mouse plasma and human plasma resulted in a significant decrease of opnurabisib response compared to the neat solution. To circumvent the effect of the biological matrices, we performed matrix effect investigations utilizing direct infusion technique. We found that the pH value has a significant effect on the response of opnurabisib when biological matrix was introduced. Our investigation indicated that mouse and human plasma showed an ion suppression at the retention of both opnurabisib and IS when they were eluted in 0.1 %  $\text{NH}_4\text{OH}$  (v/v) but not when they were eluted 0.1 % formic acid (v/v) (data not shown). Due to the lower opnurabisib response in an acidic mobile phase, a basic eluent modified with a small percentage of acid was investigated for the possible mobile phase. For this purpose, a direct infusion of 20 ng/ml opnurabisib in 25 % methanol (v/v) was introduced to the MS interface at 5  $\mu$ l/min flow rate while the isocratic flow of water modified with 0.1 %  $\text{NH}_4\text{OH}$  (v/v) and 0.01 % formic acid (v/v) (eluent A) and acetonitrile (eluent B) (50:50, v/v) was applied at 0.5 ml/min flow rate. An injection of double blank mouse plasma (lithium heparinized) did not show any ion suppression at the retention time of both opnurabisib and IS (around 0.8 min), as demonstrated by Fig. 3B. In contrast, when the same experiment was performed with 0.1 %  $\text{NH}_4\text{OH}$  (v/v) only as the modifier of eluent A, an ion suppression indicated by a decreased intensity

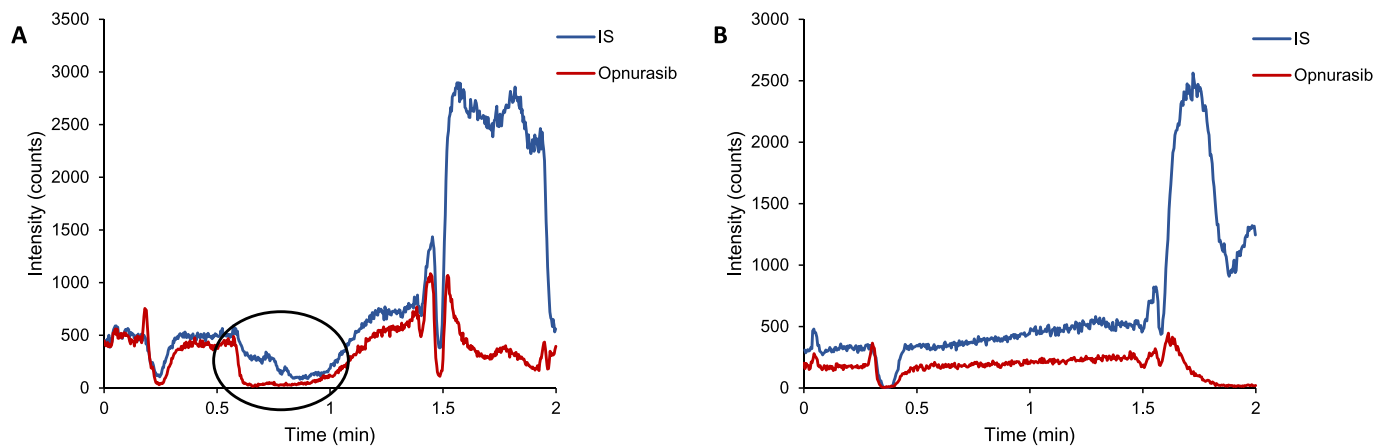
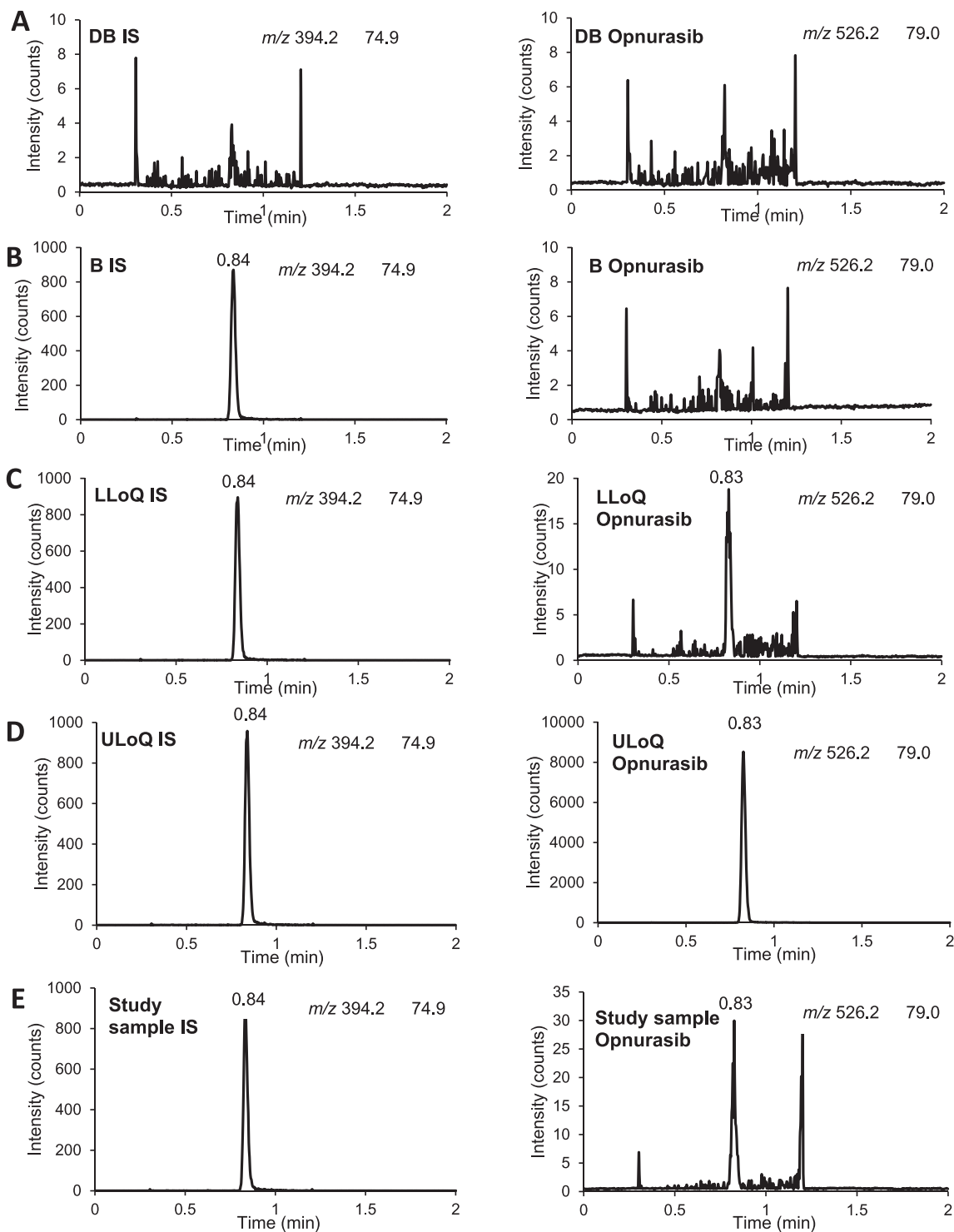


Fig. 3. The response of continuous infusion of 5  $\mu$ l/min flow rate of opnurabisib 20 ng/ml (monitored at  $m/z$  526.2  $\rightarrow$  79.0) and IS 10 ng/ml (monitored at  $m/z$  394.2  $\rightarrow$  74.9) when a double blank lithium heparin mouse plasma was injected. (A) Water modified with 0.1 %  $\text{NH}_4\text{OH}$  and acetonitrile (50:50 v/v) at 0.5 ml/min used as mobile phase. (B) Water modified with 0.1 %  $\text{NH}_4\text{OH}$  & 0.01 % formic acid and acetonitrile (50:50 v/v) at 0.5 ml/min used as mobile phase.



**Fig. 4.** Representative chromatograms of opnurasib in processed mouse plasma (A–D) and homogenates of mouse brain (E). (A) Double blank (DB), (B) Blank (B, containing 10 ng/ml IS), (C) LLoQ (containing 2 ng/ml opnurasib and 10 ng/ml IS), (D) ULoQ (containing 2000 ng/ml opnurasib and 10 ng/ml IS), (E) study sample (containing 4.6 ng/ml opnurasib and 10 ng/ml IS).

between 0.6 and 0.9 min was observed in both opnurasib and IS transitions (Fig. 3A). Therefore, we utilized water modified with 0.1 %  $\text{NH}_4\text{OH}$  (v/v) and 0.01 % formic acid (v/v) as final eluent A to validate this analytical method. Since eluent A has high pH value (pH 9.9–10.0) that is prone to pH drop due to reaction with carbon dioxide during the storage [20,21], fresh eluent A was always daily prepared before the routine use.

Since this quantification method was developed to support

preclinical studies of opnurasib in mouse, hundreds of samples with low volume of sample, *i.e.*, 10  $\mu\text{l}$  of mouse plasma were expected. Therefore, a fast and straightforward sample pretreatment was preferred. Protein precipitation as sample pretreatment was optimized because of this. Both acetonitrile and methanol were empirically tested as the precipitating agent. Acetonitrile was selected because it provided a higher response of opnurasib with less volume of organic solvent. Moreover, a 96-well plate format protein precipitation was used to enable high

**Table 2**

Selectivity data of opnurasib at QC-LLoQ level (2 ng/ml) in all investigated individual mouse matrices.

Mouse matrices	Mean measured concentration (ng/ml)	Mean area ratio* of opnurasib (%)	Mean area ratio* of erlotinib (%)	n
Plasma (lithium heparinized)	1.82 ± 0.26	6.66 ± 4.42	0.24 ± 0.35	6
Brain homogenates	2.17 ± 0.27	10.85 ± 3.41	0.10 ± 0.02	4
Liver homogenates	2.13 ± 0.20	12.25 ± 4.91	0.12 ± 0.07	4
Kidney homogenates	2.35 ± 0.29	9.20 ± 4.01	0.21 ± 0.20	4
Spleen homogenates	2.24 ± 0.42	7.93 ± 2.67	0.18 ± 0.09	4
Small intestines homogenates	1.90 ± 0.29	6.23 ± 2.60	0.11 ± 0.03	4
Small intestinal content homogenates	1.93 ± 0.20	9.68 ± 5.30	0.13 ± 0.04	4
Lung homogenates	2.02 ± 0.28	10.43 ± 5.34	0.21 ± 0.10	4
Testis homogenates	1.95 ± 0.26	13.13 ± 5.05	0.08 ± 0.07	4

\*Area ratio was calculated from the area of opnurasib or IS in the blank compared to the area at LLoQ level. The data is presented as the average concentration or area ratio ± SD.

throughput analysis.

The use of internal standard (IS), ideally stable isotope labelled compound (SIL), in a quantification method utilizing LC-MS/MS is a common practice to normalize possible phenomena occurring during sample pretreatment and quantification. Due to the lack of commercially available SIL-opnurasib, several tyrosine kinases and KRAS inhibitors were empirically investigated as the possible analog IS for opnurasib. KRAS<sup>G12C</sup> inhibitors sotorasib and adagrasib have been investigated as possible IS candidate. However, both compounds did not provide suitable retention time in the initial elution condition of opnurasib (0.1 % NH<sub>4</sub>OH (v/v) as eluent A). Adagrasib did not elute within two minutes run, while sotorasib eluted close to the dead time of the selected column. Among other tyrosine kinase inhibitors, erlotinib was selected as the analog IS since it has a similar retention time as opnurasib under the developed LC conditions and it has stable response across the investigated biological matrices. Representative chromatograms for opnurasib and IS are shown in Fig. 4.

### 3.2. Method validation

The presented method was fully validated for lithium-heparinized mouse plasma and partially validated for mouse brain, liver, spleen, kidney, lung, testis, small intestines, and small intestines content homogenates according to the guidelines of bioanalytical method validation from both EMA and US FDA [17,18].

#### 3.2.1. Selectivity

Selectivity was assessed at the QC-LLoQ level (2 ng/ml of opnurasib) in various individual matrices. The selectivity is demonstrated in Table 2. The average back-calculated concentrations across different mouse matrices were 1.82–2.35 ng/ml which are within the required 20 % deviation of nominal concentration. Moreover, the responses of attributable interfering component of opnurasib and erlotinib at QC-LLoQ level were below 15 % and 0.5 %, respectively, in all investigated mouse matrices. These percentages were lower than the guidelines requirement [17,18], confirming the selectivity of this method for opnurasib quantification in mouse plasma and eight mouse tissue-related homogenates down to 2 ng/ml.

**Table 3**

Accuracy and precision of the developed method in lithium heparinized mouse plasma.

Day	Statistics	Opnurasib			
		QC-LLoQ 2 ng/ml	QC-low 6 ng/ml	QC-medium 150 ng/ml	QC-high 1500 ng/ml
1	Intra-day				
	Mean (n = 6)	2.05	5.97	154.7	1515
	CV (%)	19.8 %	13.9 %	2.5 %	2.0 %
2	Bias (%)	2.5 %	-0.5 %	3.1 %	1.0 %
	Intra-day				
	Mean (n = 6)	2.02	5.82	161.0	1596
3	CV (%)	17.9 %	7.3 %	3.8 %	2.2 %
	Bias (%)	1.1 %	-3.0 %	7.3 %	6.4 %
	Intra-day				
1-3	Mean (n = 6)	2.04	5.79	152.3	1456
	CV (%)	10.9 %	11.0 %	4.3 %	1.4 %
	Bias (%)	1.8 %	-3.6 %	1.5 %	-2.9 %
1-3	Inter-day				
	Mean (n = 18)	2.04	5.86	156.0	1522
	CV (%)	15.6 %	10.5 %	4.2 %	4.3 %
1-3	Bias (%)	1.8 %	-2.3 %	4.0 %	1.5 %

QC = quality control, LLoQ = lower limit of quantification, CV = coefficient of variation

#### 3.2.2. Calibration curve and range

The relative response of opnurasib over erlotinib as IS showed a linear trend over the concentration range of 2–2000 ng/ml opnurasib. Thus, a linear equation is utilized for the quantification of opnurasib. The linear equation used a typical  $Y = a \cdot X + b$  form, where Y is the relative response of area opnurasib to area erlotinib, X denotes the concentration of opnurasib in ng/ml, a determines the curve's slope, and b defines the intercept of the calibration curve. The regression coefficient is expressed by the R<sup>2</sup> value, in which the inverse square of the opnurasib concentration is used as the weighting factor. The average calibration equation of nine consecutive calibration runs was  $Y = 0.056 (\pm 0.014) X + 0.0048 (\pm 0.0027)$  with  $R^2 = 0.989 (\pm 0.013)$ .

The quantification of opnurasib in mouse plasma and mouse tissue-related homogenates utilized a daily calibration equation that was run in the same analytical run as these samples.

#### 3.2.3. Accuracy and precision

The method performance on mouse plasma was demonstrated by accuracy/bias (%) and precision/CV (%) at four different QC-levels (Table 3). All calculated CV (%) and bias (%) values both intra- and inter-day were below 15 % for QC-low, -med, -high and were below 20 % for QC-LLoQ fulfilling the current guidelines requirements [17,18].

As for the method performance on different mouse tissue-related homogenates, the same strategy was applied at QC-medium level only as the partial validation of this method in those matrices. The detailed calculated bias (%) and CV (%) are reported in Table 4 which showed less than 15 % for both parameters either intra- or inter-day in all investigated tissue-related homogenates. All of these data demonstrated the reliability of the method in producing accurate and precise data when applied for measuring opnurasib in mouse plasma and eight mouse tissue-related homogenates samples.

#### 3.2.4. Matrix effect

The presence of the co-eluting matrix components may reduce or enhance the ion intensity of the analyte, possibly affecting the accuracy and precision of the assay. When the sample to be measured and the calibration samples do not have identical matrix components, i.e., in our case measuring the mouse tissue-related homogenates samples using the calibration samples of mouse plasma, the matrix effect has to be addressed properly. According to our data presented in Table 5, all the tested mouse matrices had accuracies between 89.9 %–107.6 % with a range of 2.0 %–8.3 % and 3.5 %–10.1 % of intra- and inter-individual

**Table 4**

Accuracy and precision of the developed method on mouse tissue-related matrices at QC-medium level (150 ng/ml).

Day	Statistic	Mouse-related tissue homogenates							
		Brain	Liver	Kidney	Spleen	SI	SIC	Lung	Testis
1	Intraday								
	Mean (n = 6)	156.3	159.2	161.3	148.9	154.1	142.8	147.5	151.5
	CV (%)	3.7 %	7.2 %	7.9 %	7.3 %	2.0 %	2.3 %	2.6 %	6.9 %
2	Bias (%)	4.2 %	6.2 %	7.6 %	-0.7 %	2.7 %	-4.8 %	-1.7 %	1.0 %
	Intraday								
	Mean (n = 6)	169.8	138.4	164.9	130.0	146.4	133.5	133.3	141.8
3	CV (%)	6.3 %	6.5 %	9.3 %	8.9 %	3.5 %	10.9 %	9.1 %	11.2 %
	Bias (%)	13.2 %	-7.8 %	10.0 %	-13.4 %	-2.4 %	-11.0 %	-11.1 %	-5.4 %
	Intraday								
1-3	Mean (n = 6)	151.1	130.2	148.9	137.1	165.1	133.5	148.7	148.4
	CV (%)	3.7 %	5.0 %	9.3 %	3.6 %	2.4 %	8.8 %	2.9 %	13.0 %
	Bias (%)	0.8 %	-13.2 %	-0.7 %	-8.6 %	10.1 %	-11.0 %	-0.9 %	-1.1 %
1-3	Inter-day								
	Mean (n = 18)	159.1	142.6	158.4	138.6	155.2	136.6	143.2	147.3
	CV (%)	6.9 %	10.7 %	9.4 %	8.7 %	5.7 %	8.2 %	7.1 %	10.4 %
	Bias (%)	6.1 %	-4.9 %	5.6 %	-7.6 %	3.5 %	-8.9 %	-4.6 %	-1.8 %

SI = small intestines, SIC = small intestinal content.

**Table 5**

Matrix effect of individual mouse matrices on opnurasib at QC-low (6 ng/ml) and -high level (1500 ng/ml).

Mouse matrices	Mean calculated concentration (ng/ml)	Accuracy (%)	Intra-individual precision (%)	Inter-individual precision (%)	n*
Plasma	5.71 ± 0.59	95.2	7.5	10.1	6
	1614 ± 77	107.6	3.3	4.7	6
Brain homogenates	5.79 ± 0.46	96.5	7.3	7.7	4
	1457 ± 64	97.2	2.0	4.2	4
Liver homogenates	6.09 ± 0.54	101.5	7.2	8.6	4
	1409 ± 83	93.9	4.1	5.7	4
Kidney homogenates	6.35 ± 0.39	105.9	4.4	6.0	4
	1574 ± 76	104.9	4.2	4.7	4
Spleen homogenates	6.15 ± 0.45	102.5	6.2	7.1	4
	1417 ± 71	94.5	2.6	4.8	4
Small intestines homogenates	6.17 ± 0.45	102.9	5.9	7.0	4
	1583 ± 87	105.5	2.6	5.3	4
Small intestinal content homogenates	5.65 ± 0.43	94.1	6.1	7.5	4
	1349 ± 93	89.9	5.5	6.7	4
Lung homogenates	6.07 ± 0.37	101.2	4.1	6.0	4
	1388 ± 73	92.5	3.7	5.1	4
Testis homogenates	6.05 ± 0.57	100.8	8.3	9.1	4
	1401 ± 50	93.4	2.6	3.5	4
Hemolyzed mouse plasma (pooled)	5.85 ± 0.67	97.5	11.4		1
	1503 ± 20	100.2	1.4		

\* n = the number of investigated individual sources. Mean calculated concentration reported the average of 24 data (plasma) and 16 data (each tissue homogenates, except for brain was 15 data) ± SD.

precisions, respectively, for both QC-high and QC-low level. These data indicate that there is no significant matrix effect in both mouse plasma and mouse-tissue related homogenates interfering with the quantification of opnurasib in this developed assay.

The effect of hemolyzed plasma in pooled matrix was investigated as the worst scenario if hemolysis happens during the blood withdrawal while the effect of lipemic plasma was not investigated because we did not expect to receive such samples due to the controlled diet of the mice used in this study. The accuracy and precision data of the hemolyzed plasma sample (Table 5) demonstrated that there is no significant matrix effect hampering the measurement of opnurasib in hemolyzed plasma sample.

### 3.2.5. Recovery & carry-over

The recovery of opnurasib and IS was determined at QC-low, -medium, and -high level in both mouse and human lithium heparin plasma. We also investigated the recovery in human plasma because we used human plasma to dilute some of our preclinical samples to fit the calibration range. Opnurasib had a range of % recovery of 93.4 %–103.5 % and 99.3 %–104.3 % for mouse and human plasma, respectively, while in the same order IS had a range of 101.6 %–106.7 % and 100.9 %–

101.7 % in all investigated QC levels. With % recovery value being around 100 % for both analyte and IS in both human and mouse plasma, we showed that there is no significant loss of the analytes and IS during the protein precipitation utilized in this method potentially hampering the sensitivity of this assay.

The injection of blank and double blank samples right after the highest calibration sample showed a slightly over 20 % response of the QC-LLoQ samples. However, this response decreased down to less than 20 % after the second blank injection. Therefore, we always put at least two blank or double blank samples after the expected high concentration samples.

### 3.2.6. Dilution integrity

Dilution integrity was determined to accommodate some preclinical samples that have a concentration over the upper limit of quantification (ULOQ, 2,000 ng/ml). According to our experience, this is likely to happen due to the possibility of the high tissue concentration in some tissues. The selected dilution factors to be validated were 5-, 10-, 11-, and 51-fold. All the dilution was performed utilizing lithium heparin human plasma (pooled gender). The bias (%) and CV (%) were reported as 11.2 % and 1.8 % (5-fold), 11.4 % and 2.6 % (10-fold), 11.3 % and



**Table 6**

Stability of opnurasib in different mouse matrices (reported as the mean of percentage of the recovered concentrations  $\pm$  SD, n = 4 for each concentration on each exposure condition).

Mouse matrix	Exposure conditions	QC level	Conc. (ng/ml)	Stability (%)
Plasma (lithium heparinized)	12 h at RT	QC-low	6	101.5 $\pm$ 10.2
		QC-high	1500	93.4 $\pm$ 6.3
	three freeze thaw cycle 3 months at -30 °C	QC-low	6	98.8 $\pm$ 5.2
		QC-high	1500	87.7 $\pm$ 4.4
		QC-low	6	85.1 $\pm$ 15.2
Brain homogenates	8 h at RT	QC-high	1500	95.7 $\pm$ 1.5
		QC-medium	150	86.7 $\pm$ 6.5
Liver homogenates	8 h at RT	QC-medium	150	91.1 $\pm$ 1.4
Kidney homogenates	8 h at RT	QC-medium	150	78.9 $\pm$ 9.4
	4 h at RT	QC-medium	150	87.8 $\pm$ 3.6
	5 h on iced condition	QC-medium	150	86.5 $\pm$ 10.0
Spleen homogenates	8 h at RT	QC-medium	150	89.6 $\pm$ 8.3
Small intestines homogenates	8 h at RT	QC-medium	150	97.7 $\pm$ 3.0
Small intestinal content homogenates	8 h at RT	QC-medium	150	86.9 $\pm$ 11.0
Lung homogenates	8 h at RT	QC-medium	150	86.4 $\pm$ 1.7
Testis homogenates	8 h at RT	QC-medium	150	96.1 $\pm$ 12.2
		QC-high	1500	100.4 $\pm$ 3.6
		QC-medium	150	86.1 $\pm$ 4.9
Whole blood (lithium heparinized)	2 h at RT	QC-high	1500	104.7 $\pm$ 8.9
		QC-medium	150	88.5 $\pm$ 2.6
		QC-high	1500	88.5 $\pm$ 2.6

QC = quality control, Conc. = concentration, RT = room temperature.

2.3 % (11-fold), and lastly 14.4 % and 2.8 % (51-fold) demonstrated the accuracy and precision of these dilution factors.

### 3.2.7. Stability

The stability of opnurasib in the investigated mouse matrices is

presented in Table 6. Opnurasib in mouse plasma is stable up to 12 h at a room temperature, up to 3 months when the sample is stored at -30 °C and after three cycles of freezing and thawing the sample. In most of the investigated tissue-related homogenates, opnurasib is stable up to 8 h at ambient temperature. However, opnurasib showed a rather short-lasting stability at room temperature in kidney homogenates, only up to 4 h, which is shorter than in other tissue-related homogenates. Therefore, we also tested the stability of opnurasib in mouse kidney homogenates on an ice condition. We showed that on an iced condition, opnurasib in kidney homogenates was stable up to 5 h. In relation to this matter, preparation of kidney homogenates samples on iced condition should be considered. This may be driven by a possibility of the affinity of opnurasib with the urea transporter in kidney due to the presence of acrylamide which is an urea analogue [22].

The stability of opnurasib in whole blood was investigated at several time points and the results are illustrated in Fig. 5. The graph shows that opnurasib in whole blood was stable up to 2 h at room temperature and up to 5 h on iced condition (refer to Table 6 for % recovered after the mentioned exposure conditions). This information needs to be taken into consideration when handling mouse blood during a mouse study, including blood withdrawal and processing into plasma.

The reanalysis of processed samples at QC-low and -high were performed one week after a storage at multisampler temperature. The bias (%) and CV (%) for QC-high were 92.0 % and 2.4 % respectively, while for QC-low these values were 99.2 % and 9.9 %. The data demonstrate that opnurasib in processed samples was stable up to 7 days after storage at 4 °C, allowing us to do a reliable processed sample remeasurement within that period. Opnurasib stock solution (in methanol) and working solution (in 50 % methanol, v/v) showed a stable response compared to freshly prepared stock and working solutions after storage at -30 °C for 4 months and after exposure at room temperature for 6 h (Table 7).

**Table 7**

Stability of opnurasib stock and working solutions (reported as the percentage of the response of freshly prepared solution, n = 2).

Conditions	Stability (%)
Working solution* after 6 h at RT	104.2
Working solution* after 4 months at -30 °C	110.9
Stock solution** after 6 h at RT	98.1
Stock solution** after 4 months at -30 °C	97.2

\*Working solution was prepared in 50 % methanol (v/v), \*\*stock solution was prepared in methanol, RT = room temperature.

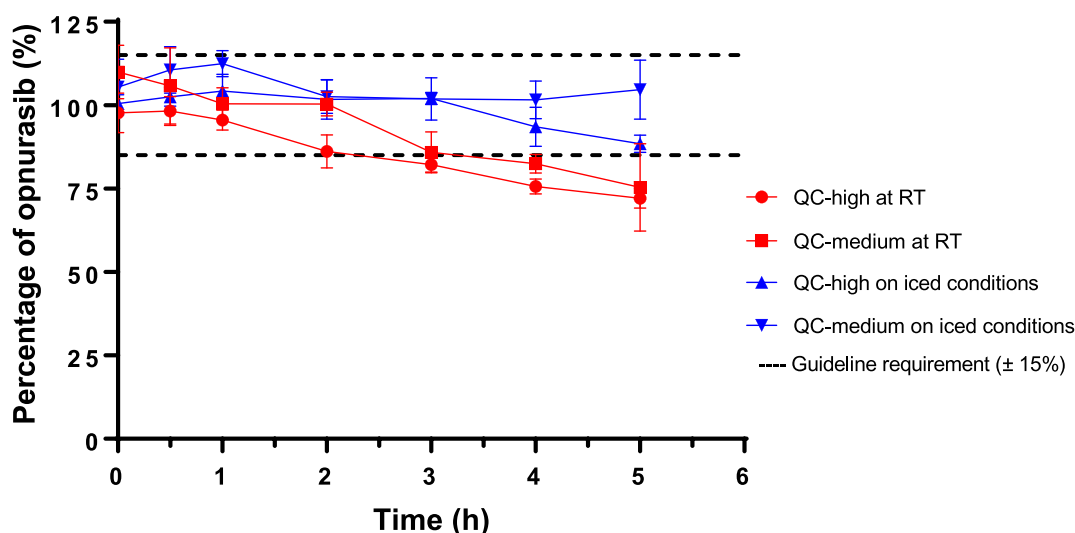


**Fig. 5.** The percentage of remaining opnurasib in mouse whole blood samples compared to nominal concentrations after exposure to room temperature and iced conditions for 5 h. QC-high = 1500 ng/ml opnurasib, QC-medium = 150 ng/ml opnurasib, RT = room temperature.

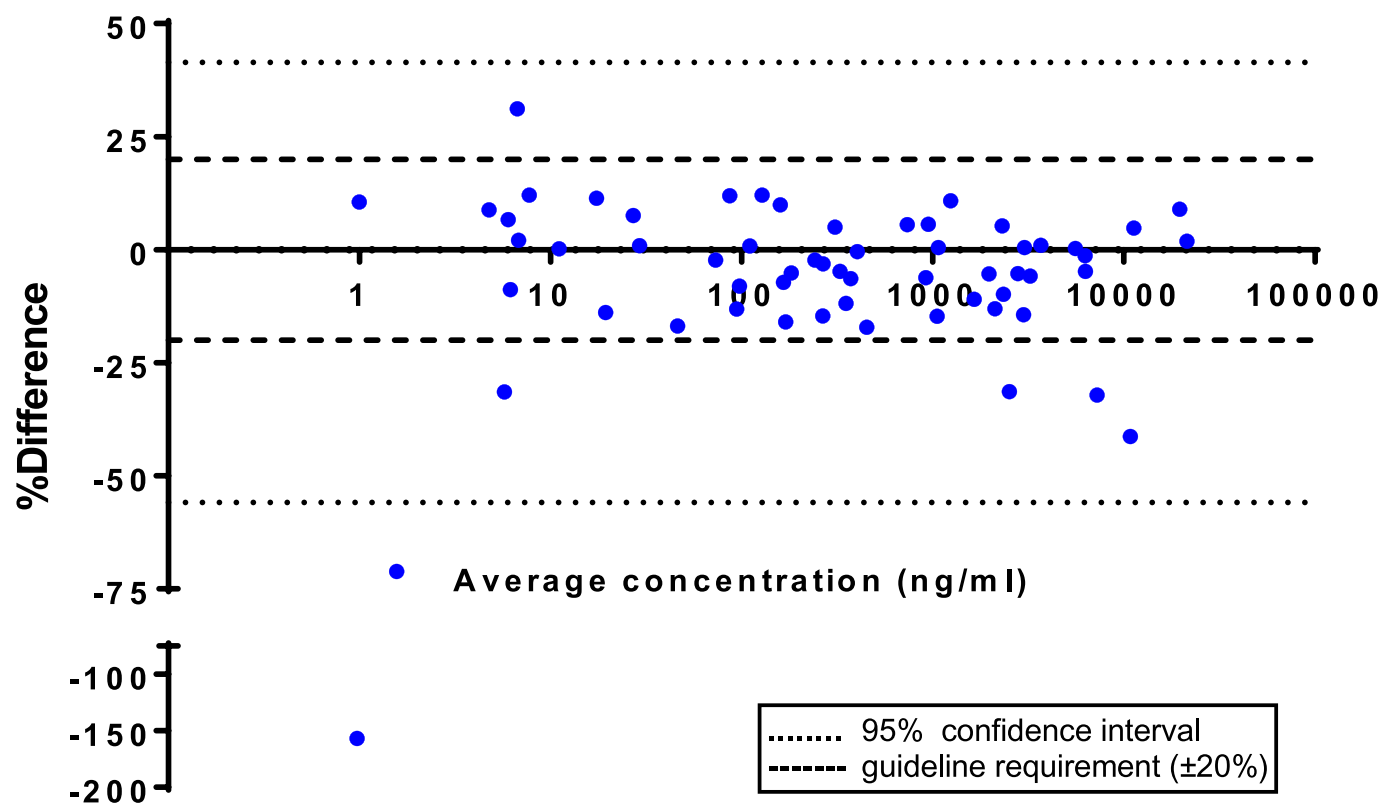


Fig. 6. Bland Altman plot of two different measurements of sixty preclinical samples. Average concentration is the mean concentration of two measurements of the same sample. The difference (%) describes the percentage of the difference between two measurements of the same sample against the average concentration of those measurements.

### 3.2.8. Incurred samples reanalysis

To verify the reliability of the reported sample concentration from preclinical samples, reanalysis of some preclinical samples was performed one week after the initial measurement. The incurred sample reanalysis (ISR) of a total 60 preclinical samples resulted in 53 out of 60 samples producing  $< 20\%$  differences between initial and ISR measurements. This number is in line with the guidelines requirement that stipulates at least 40 out of 60 samples should have differences within  $\pm 20\%$  between two measurements [17,18]. The detailed data on ISR is presented in Fig. 6. The extreme outlier value was possibly owing to its calculated concentrations that are lower than the established LLOQ.

### 3.3. Blood-to-plasma concentration ratio ( $R_b$ )

The  $R_b$  was determined by calculating the ratio of back-calculated concentration of mouse WB samples over mouse plasma-derived samples ( $n = 4$ ). The obtained average  $R_b$  was 1.02 with a standard deviation of 0.04. The value of 1.02 illustrated the equal distribution of opnurabis between mouse plasma and mouse red blood cells. This information demonstrated that the measured plasma concentration of opnurabis is a good representation of its systemic concentration in mouse.

### 3.4. Preclinical study

The validated method was utilized to measure opnurabis concentrations in mouse plasma and mouse tissue homogenates in a pilot pharmacokinetic mouse study. This pilot study was performed in six male wild-type mice (FVB genetic background) that received orally administered opnurabis at 30 mg/kg body weight. This pilot study has a total 8 h study duration. The mouse plasma concentration over time curve of the six mice is illustrated in Fig. 7. The curve clearly showed that the  $C_{max}$  of opnurabis is achieved around 1 h after the oral

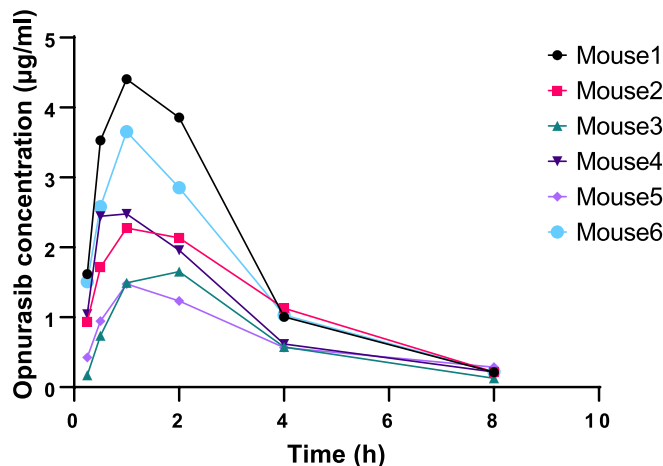


Fig. 7. Plasma concentration over time curve of opnurabis in six male wild-type mice administered with 30 mg/kg bodyweight of opnurabis.

administration. The calculated pharmacokinetic parameters obtained from plasma concentration were:  $C_{max} = 2.66 \pm 1.15 \mu\text{g/ml}$ ,  $T_{max} = 1.17 \pm 0.41 \text{ h}$ ,  $T_{1/2} = 1.91 \pm 0.50 \text{ h}$ ,  $K_e = 0.38 \pm 0.07 \text{ h}^{-1}$ ,  $AUC_{0 \rightarrow 8} = 9.3 \pm 3.4 \mu\text{g}\cdot\text{h}\cdot\text{ml}^{-1}$ , &  $AUC_{0 \rightarrow \infty} = 9.9 \pm 3.3 \mu\text{g}\cdot\text{h}\cdot\text{ml}^{-1}$ .

The tissue concentration of opnurabis in several investigated tissue-related matrices was calculated and presented in Fig. 8. The graph showed that the brain has the lowest opnurabis concentration compared to the other investigated tissues, perhaps due to the presence of the blood brain barrier. Besides brain, testis also showed a low opnurabis distribution illustrating the possibility of a low risk of opnurabis teratogenicity in males. In contrast, the highest distribution of opnurabis 8 h

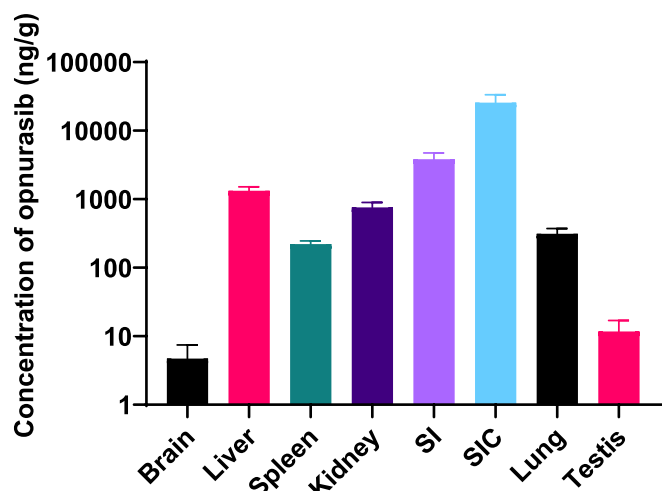


Fig. 8. Opnurabisib concentration in mouse tissue ( $n = 6$  for each tissue) 8 h after a single dose administration of opnurabisib (30 mg/kg). The graph was plotted in a logarithmic scale. SI = small intestines. SIC = small intestinal content.

after a single dose of opnurabisib was observed in small intestinal content. This high concentration may be caused by a possible affinity of opnurabisib for intestinal efflux transporter.

#### 4. Conclusions

A reliable bioanalytical method utilizing LC-MS/MS to quantify KRAS<sup>G12C</sup> inhibitor opnurabisib in mouse plasma and mouse tissue related homogenates has been successfully developed and validated. The reported method was capable to reliably measure opnurabisib down to 2 ng/ml in 10- $\mu$ l samples volume with a straight-forward protein precipitation as sample pretreatment in a 96-well plate format. The accuracy and precision of this method at all investigated levels and in all tested mouse matrices were within the latest guideline requirements. The absence of a significant matrix effect and extraction loss that possibly hampered opnurabisib quantification in investigated matrices was successfully demonstrated. Finally, this validated method has been successfully applied to support a mouse pharmacokinetic and tissue distribution study, and therefore it can be used further to support similar preclinical studies in the near future.

#### CRediT authorship contribution statement

**Irene A. Retmana:** Conceptualization, Methodology, Validation, Formal analysis, Investigation, Visualization, Writing – original draft. **Nefise Çelebi:** Validation, Formal analysis, Writing – review & editing. **Jamie Rijmers:** Formal analysis, Investigation, Writing – review & editing. **Alfred H. Schinkel:** Conceptualization, Resources, Writing – review & editing, Supervision. **Jos H. Beijnen:** Conceptualization, Resources, Writing – review & editing, Supervision. **Rolf W. Sparidans:** Conceptualization, Methodology, Resources, Writing – review & editing, Supervision.

#### Declaration of competing interest

The authors declare that they have no known competing financial interests or personal relationships that could have appeared to influence the work reported in this paper.

#### Data availability

Data will be made available on request.

#### References

- [1] F. Sanchez-Vega, M. Mina, J. Armenia, et al., Oncogenic signaling pathways in the cancer genome atlas, *Cell* 173 (2018) 321–337.e10, <https://doi.org/10.1016/J.CELL.2018.03.035>.
- [2] A.D. Cox, S.W. Fesik, A.C. Kimmelman, et al., Drugging the undruggable RAS: mission possible? *Nat. Rev. Drug Discov.* 13 (2014) 828–851, <https://doi.org/10.1038/nrd4389>.
- [3] B. El Osta, M. Behera, S. Kim, et al., Characteristics and outcomes of patients with metastatic KRAS-mutant lung adenocarcinomas: The Lung Cancer Mutation Consortium Experience, *J. Thorac. Oncol.* 14 (2019) 876–889, <https://doi.org/10.1016/j.jtho.2019.01.020>.
- [4] S.Y. Liu, H. Sun, J.Y. Zhou, et al., Clinical characteristics and prognostic value of the KRAS G12C mutation in Chinese non-small cell lung cancer patients, *Biomark. Res.* 8 (2020) 22, <https://doi.org/10.1186/s40364-020-00199-z>.
- [5] J.M. Ostrem, U. Peters, M.L. Sos, et al., K-Ras(G12C) inhibitors allosterically control GTP affinity and effector interactions, *Nat.* 503 (2013) 548–551, doi: 10.1038/NATURE12796.
- [6] M.R. Janes, J. Zhang, L.S. Li, et al., Targeting KRAS mutant cancers with a covalent G12C-specific inhibitor, *Cell* 172 (2018) 578–589.e17, <https://doi.org/10.1016/J.CELL.2018.01.006>.
- [7] S.Y. Nakajima, N. Drezner, X. Li, et al., FDA approval summary: Sotorasib for KRAS G12C-mutated metastatic NSCLC, *Clin. Cancer Res.* 28 (2022) 1482–1486, <https://doi.org/10.1158/1078-0432.CCR-21-3074>.
- [8] S. Dhillon, Adagrasib: first approval, *Drugs* 83 (2023) 275–285, <https://doi.org/10.1007/s40265-023-01839-Y>.
- [9] H. Wang, L. Chi, F. Yu, et al., Annual review of KRAS inhibitors in 2022, *Eur. J. Med. Chem.* 249 (2023), 115124, <https://doi.org/10.1016/J.EJMECH.2023.115124>.
- [10] A.I. Fernández-Llamazares, X. Bofill, P. Cole, European Federation of Medicinal Chemistry - XXVI International Symposium on Medicinal Chemistry (EFMC-ISMCh 2021), *Drugs Future* 46 (2021) 937–950, <https://doi.org/10.1358/DOF.2021.46.11.3367670>.
- [11] A. Weiss, E. Lorthiois, L. Barys, et al., Discovery, preclinical characterization, and early clinical activity of JDQ443, a structurally novel, potent, and selective covalent oral inhibitor of KRASG12C, *Cancer Discov.* 12 (2022) 1500–1517, <https://doi.org/10.1158/2159-8290.CD-22-0158>.
- [12] E. Lorthiois, M. Gerspacher, K.S. Beyer, et al., JDQ443, a structurally novel, pyrazole-based, covalent inhibitor of KRASG12C for the treatment of solid tumors, *J. Med. Chem.* 65 (2022) 16173–16203, <https://doi.org/10.1021/acs.jmedchem.2c01438>.
- [13] Study of JDQ443 in Patients with Advanced Solid Tumors Harboring the KRAS G12C Mutation (KontraSt-01), (n.d.), <https://clinicaltrials.gov/study/NCT04699188?term=JDQ443&rank=3> (accessed August 1, 2023).
- [14] P.A. Cassier, C.A. Dooms, A. Gazzah, et al., KontraSt-01 update: Safety and efficacy of JDQ443 in KRAS G12C-mutated solid tumors including non-small cell lung cancer (NSCLC), *J. Clin. Oncol.* 41 (2023), 9007, <https://doi.org/10.1200/JCO.2023.41.16.suppl.9007>.
- [15] C.J. Lucas, J.H. Martin, Pharmacokinetic-guided dosing of new oral cancer agents, *J. Clin. Pharmacol.* 57 (2017) S78–S98, <https://doi.org/10.1002/jcph.937>.
- [16] T. Hendrayana, A. Wilmer, V. Kurth, et al., Anticancer dose adjustment for patients with renal and hepatic dysfunction: from scientific evidence to clinical application, *Sci. Pharm.* 85 (2017), <https://doi.org/10.3390/scipharm85010008>.
- [17] European Medicines Agency, ICH guideline M10 on bioanalytical method validation and study sample analysis, 2022, [https://www.ema.europa.eu/en/documents/scientific-guideline/ich-guideline-m10-bioanalytical-method-validation-step-5\\_en.pdf](https://www.ema.europa.eu/en/documents/scientific-guideline/ich-guideline-m10-bioanalytical-method-validation-step-5_en.pdf) (accessed January 31, 2023).
- [18] Fda, Cder, M10 BIOANALYTICAL METHOD VALIDATION AND STUDY SAMPLE ANALYSIS Guidance for Industry, 2022, <https://www.fda.gov/vaccines-blood-biologics/guidance-compliance-regulatory-information-biologics/biologics-guidances> (accessed June 27, 2023).
- [19] Y. Zhang, M. Huo, J. Zhou, et al., PKSolver: an add-in program for pharmacokinetic and pharmacodynamic data analysis in Microsoft Excel, *Comput. Methods Programs Biomed.* 99 (2010) 306–314.
- [20] I.A. Retmana, N.H.C. Loos, A.H. Schinkel, et al., Quantification of KRAS inhibitor sotorasib in mouse plasma and tissue homogenates using liquid chromatography-tandem mass spectrometry, *J. Chromatogr. B. Analyt. Technol. Biomed. Life Sci.* 1174 (2021), doi: 10.1016/J.JCHROMB.2021.122718.
- [21] A. Tan, J.C. Fanaras, Use of high-pH (basic/alkaline) mobile phases for LC-MS or LC-MS/MS bioanalysis, *Biomed. Chromatogr.* 33 (2019) e4409.
- [22] B. Yang, Transport characteristics of urea transporter-BB. Yang, J.M. Sands (Eds.), in: *Urea Transp*, Springer, Dodrecht, 2014, pp. 127–135, [https://doi.org/10.1007/978-94-017-9343-8\\_8](https://doi.org/10.1007/978-94-017-9343-8_8).